Submitted to ApJ
Preprint typeset using LaTeX style emulateapj v. 04/21/05

arXiv:astro-ph/0601629v2 26 Jul 2006

# LOW RADIATIVE EFFICIENCY ACCRETION AT WORK IN ACTIVE GALACTIC NUCLEI: THE NUCLEAR SPECTRAL ENERGY DISTRIBUTION OF NGC 4565

M. Chiaberge[1]
Space Telescope Science Institute, 3700 San Martin Dr., Baltimore, MD 21218

R. Gilli[2]
INAF - Osservatorio astronomico di Bologna, Via Ranzani 1, 40127 Bologna, Italy

F. D. Macchetto[3]
Space Telescope Science Institute, 3700 San Martin Dr., Baltimore, MD 21218

and

William B. Sparks
Space Telescope Science Institute, 3700 San Martin Dr., Baltimore, MD 21218

*Submitted to ApJ*

## ABSTRACT

We derive the spectral energy distribution (SED) of the nucleus of the Seyfert galaxy NGC 4565. Despite its classification as a Seyfert 2, the nuclear source is substantially unabsorbed. The absorption we find from Chandra data ($N_H = 2.5 \times 10^{21}$ cm$^{-2}$) is consistent with that produced by material in the galactic disk of the host galaxy. HST images show a nuclear unresolved source in all of the available observations, from the near-IR H band to the optical U band. The SED is completely different from that of Seyfert galaxies and QSO, as it appears basically “flat” in the IR-optical region, with a small drop-off in the U-band. The location of the object in diagnostic planes for low luminosity AGNs excludes a jet origin for the optical nucleus, and its extremely low Eddington ratio $L_o/L_{Edd}$ indicates that the radiation we observe is most likely produced in a radiatively inefficient accretion flow (RIAF). This would make NGC 4565 the first AGN in which an ADAF-like process is identified in the optical. We find that the relatively high [OIII] flux observed from the ground cannot be all produced in the nucleus. Therefore, an extended NLR must exist in this object. This may be interpreted in the framework of two different scenarios: i) the radiation from ADAFs is sufficient to give rise to high ionization emission-line regions through photoionization, or ii) the nuclear source has recently “turned-off”, switching from a high-efficiency accretion regime to the present low-efficiency state.

*Subject headings:* galaxies: active — galaxies: nuclei — accretion, accretion disks — galaxies: individual (NGC 4565)

## 1. INTRODUCTION

Low luminosity active galactic nuclei (LLAGN) are believed to be powered by accretion of matter onto the central supermassive black hole, similarly to powerful AGN. In a large fraction of LLAGN, the central black hole is as massive as in powerful distant quasars ($M_{BH} \sim 10^8 - 10^9 M_\odot$), thus their very low nuclear luminosity implies that accretion occurs with very low radiative efficiency (or at very low rates; see e.g. Ho 2004; Chiaberge et al. 2005). If so, the physics of the accretion process may be different from the “standard” optically thick, geometrically thin accretion disks. Starting from the “ion-supported tori” of Rees et al. (1982), a number of theoretical models have been developed to describe such radiatively inefficient accretion flows (RIAF, e.g. advection-dominated accretion flows, ADAF, advection-dominated inflow-outflow solutions, ADIOS, convection-dominated accretion flows, CDAF Narayan & Yi 1994; Quataert & Narayan 1999; Abramowicz et al. 2002). But because of the very low radiation they emit at all wavelengths, these objects (if they at all exist) are very difficult to be observed. Recently, the AGN nature of optical nuclear components seen in HST images of a sample of LLAGN have been unambiguously established. Maoz et al. (2005) have shown that among a sample of 17 LLAGN, 15 of them show variability over a timescale of a few months, which demonstrate their non–stellar origin. However, it is still unclear whether the radiation is from a jet or from the accretion flow. LLAGN have also been found to lie on the so-called “fundamental plane of black hole activity” (Merloni et al. 2003; Falcke et al. 2004), which attempts to unify the emission from all sources around black holes, over a large range of masses and luminosities, from Galactic sources to powerful quasars. But the origin of such a “fundamental plane” and its relationship with the origin of the radiation is still a matter of debate (e.g Bregman 2005; Koerding et al. 2006).

RIAF models have been applied to several sources belonging to different classes, such as low-luminosity radio galaxies, “normal” ellipticals, the Galactic cen-

---

Electronic address: chiab@stsci.edu

[1] On leave from INAF, Istituto di Radioastronomia, via P. Gobetti 101, I-40129 Bologna

[2] Visiting Programmer, Space Telescope Science Institute

[3] On assignment from ESA

ter Sagittarius A (e.g. Quataert & Narayan 1999; Di Matteo et al. 2000, 2003). However, for most of these objects, the models cannot be properly constrained, mostly because the nuclear radiation is swamped by other processes. This is particularly problematic in the optical band, which appears to be crucial to fix the models, where the stellar emission from the host galaxy is substantial. It is indeed in the IR-to-UV region that different accretion disk models are expected to show the largest difference in spectral shape. RIAFs should lack both the "big blue-bump" and the IR (reprocessed) bump, which instead characterize optically thick, geometrically thin accretion disk emission and the surrounding heated dust. For example, in low luminosity radio galaxies non-thermal emission from the jet dominates the optical nuclear radiation (Chiaberge et al. 1999), while the Galactic center is not visible in the optical because it is hidden by a large amount of dust.

Therefore, neither of the above mentioned classes of objects appear to be suitable laboratories to test models of low-efficiency accretion through the analysis of their overall SED. Recently, among LLAGN which show very low Eddington ratios $L_{bol}/L_{Edd} << 10^{-3}$, Chiaberge et al. (2005) have found that a class of LLAGN, mainly composed by LINERs and low-luminosity Seyfert 1 galaxies, show faint optical unresolved nuclei in HST images that may be interpreted as direct radiation from a very low efficiency accretion flow. In fact, when the radio-optical properties of LLAGN are considered, Seyfert, LINERs and low luminosity radio galaxies separate into different regions of diagnostic planes, according to the properties of their nuclei. If this interpretation is correct, we now have a powerful tool to identify the nature of the nuclear radiation (i.e. jet-dominated or accretion-dominated). The best possibility of detecting radiation from an ADAF-like process would then be to study unobscured Seyferts of lowest luminosity, as well as a sub-class of LINERs. In all other objects other radiation processes dominate.

In this paper we further test the picture outlined in Chiaberge et al. (2005) by studying the nuclear spectral energy distribution of a galaxy, NGC 4565, that seems to be a perfect candidate for hosting a RIAF around the central supermassive black hole. The object is part of the "Palomar sample" of LLAGN (Ho et al. 1997a), and it is included in both the Merloni et al. (2003) and Falcke et al. (2004) samples that were used to define the "fundamental plane of black hole activity". It is worth mentioning that NGC 4565 does not show any significant peculiarity in that plane. NGC 4565 is a nearby (d=9.7 Mpc) LLAGN classified as a Seyfert 1.9 because of the possible presence of a faint, relatively broad (FWHM = 1750 km s$^{-1}$) H$\alpha$ line. However, as Ho et al. (1997b) have pointed out, the detection of a broad component is highly uncertain. As we show in the following, although it is a Type 2 Seyfert, this object is only moderately absorbed, and the nuclear radiation is visible in the optical spectral region. NGC 4565 may thus represent the first clear example of low-luminosity accretion onto a supermassive black hole in the optical band.

In Section 2 we describe the *Chandra* and *HST* observations, the data analysis procedures and flux measurements, in Section 3 we present the results, we derive the spectral energy distribution and we discuss its interpretation. In Section 4 we give a summary of our findings and we draw conclusions.

## 2. OBSERVATIONS AND DATA ANALYSIS

We use X-ray data taken with Chandra satellite, and IR through optical HST images. In the following we describe the data and the analysis procedures.

### 2.1. *Chandra data*

A 60 ksec ACIS-S observation of NGC 4565 (performed in 2003, PI D. Wang) is publicly available in the *Chandra* archive. We retrieve the *Chandra* data and analyze them using standard CIAO 3.2.2 procedures, applying the latest calibration files in the CALDB 3.1.0 database. The X-ray image reveals a wealth of pointlike sources, many of which located along the NGC 4565 disk. The two brightest sources correspond to an off-nuclear source at ∼ 50 arcsec from the nucleus, and to the nucleus itself (see also the XMM image in Foschini et al. 2002).

To avoid contamination from faint nearby X-ray sources, the 0.4-7 keV nuclear spectrum is extracted in a circular aperture of 6 pixel radius (∼ 3 arcsec, corresponding to an encircled energy fraction of > 97% at 1.5 keV). The background is evaluated in a large annulus around the nucleus. Faint X-ray sources are not masked out from the background region, since their presence has a negligible impact on our results (the total background flux including faint sources is less than 1% of the nuclear flux). Given the moderate nuclear count rate (0.036 counts/sec), X-ray photon pileup is under control ($\lesssim 4\%$).

Spectral analysis is carried out with XSPEC v11.3.1, with the column density of our Galaxy fixed to 1.3 $10^{20}$ cm$^{-2}$ (Dickey & Lockman 1990). The spectrum is rebinned to have at least 20 photons per bin to allow use of the $\chi^2$ statistics, errors are quoted at the 90% c.l. for one interesting parameter. We find that an absorbed power law model provides a very good description of the data ($\chi^2/dof = 51/81$), the best fit photon index and column density being $\Gamma = 1.91^{+0.22}_{-0.19}$ and $N_H = 2.5 \pm 0.6$ $10^{21}$ cm$^{-2}$, respectively. The observed source fluxes in the 0.5-2 keV (soft) and 2-10 keV (hard) bands are 9.0 $10^{-14}$ erg cm$^{-2}$ s$^{-1}$ and 2.1 $10^{-13}$ erg cm$^{-2}$ s$^{-1}$, respectively. When corrected for absorption, these correspond to intrinsic nuclear luminosities of 1.9 $10^{39}$ erg s$^{-1}$ and 2.5 $10^{39}$ erg s$^{-1}$ in the soft and hard band, respectively. We note that the derived X-ray spectral parameters, fluxes and luminosities are in good agreement with those measured in a 14 ksec XMM-*Newton* observation performed in 2001 (Cappi et al. 2006).

### 2.2. *HST data*

HST data are available in the MAST archive at STScI from the near IR to the optical U-band. Images were taken as part of different programs, with the following instruments and filters: NICMOS (F160W), WFPC2 (F814W, F555W, F450W), ACS/HRC (F330W). These filters approximate the H,I,V,B and U bands in the HST system. The images are processed with the standard on-the-fly reprocessing calibration pipeline (see Pavlosky 2005).

The optical images show the bulge of the galaxy partially covered by a prominent dust lane or disk seen almost edge-on (Fig. 1) The inclination of the "disk" is

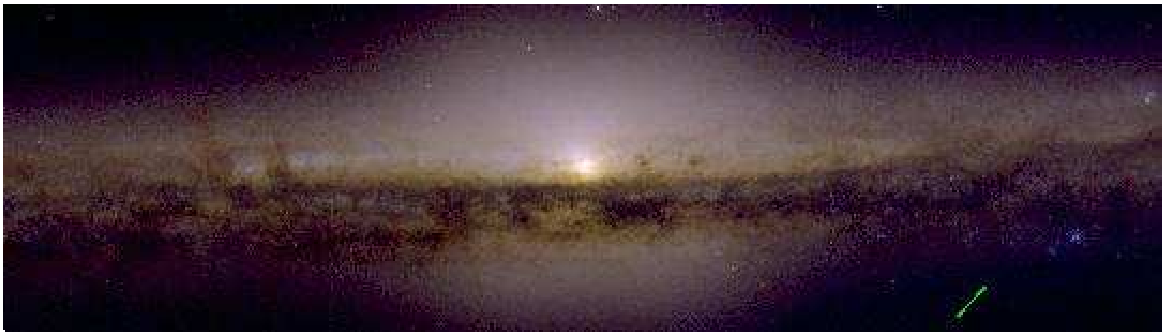

Fig. 1.— HST WFPC2 "true-color" RGB image. The R-channel corresponds to the F814W filter, the B-channel is the F450W and the G-channel is the average of the two filters. Direction to the North is indicated by the arrow.

TABLE 1
Nuclear fluxes from HST observations

| Instrument/Filter | $T_{exp}$ [s] | Program ID | Wavelength [Å] | $F_\lambda$ |
|---|---|---|---|---|
| ACS-HRC/F330W | 1200 | 9379 | 3367 | 8.1 |
| WFPC2/F450W | 600 | 6092 | 4575 | 18 |
| WFPC2/F555W | 320 | 6685 | 5468 | 21 |
| WFPC2/F814W | 480 | 6092 | 8023 | 11 |
| NICMOS/F160W | 384 | 7331 | 16074 | 5.9 |

Note. — Fluxes (in units of $10^{-17}$ erg $\mathrm{cm}^{-2}\mathrm{s}^{-1}$ Å$^{-1}$) have been corrected for local extinction using $N_H = 2.5 \times 10^{21} cm^{-2}$ and standard $A_V/N_H = 5 \times 10^{-22}$ ratio.

such that the central region of the bulge is not covered by a large amount of dust, and a faint nuclear compact source (to which we refer as the *nucleus*) is visible in all images.

### 2.2.1. *Nuclear photometry*

In the U-band, the emission from the bulge stars is low, and the nucleus is the by far the brightest source in the field of view of the ACS/HRC (Fig. 3). Photometry of the nucleus is thus straightforward in the U-band, also thanks to the higher resolution, smaller projected pixel-size of the HRC. On the other hand, in the IR (NICMOS) and optical I,V and B band WFPC2 images (the target is always located in one of the WF cameras) the contrast with the underlying stellar background is low, thus the measurement of the nuclear flux is more problematic. For the photometry of nuclear unresolved sources superimposed to the stellar emission of the host galaxy, we undertake two different approaches, as described in the following.

1) Aperture photometry with the *IRAF* task *radprof*, measuring the background close to the unresolved nucleus, at a distance of $\sim 0.4''$ from the center of the point source, and setting the aperture radius at the same distance. Note that the "background" here is the stellar emission of the galaxy in the vicinity of the nucleus. Therefore, this approach works well for nuclei in elliptical galaxies with flat radial brightness profiles, i.e. Nuker-law "core" galaxies (Faber et al. 1997) which have a flat ($\gamma < 0.3$, $\Sigma \propto r^{-\gamma}$, where $\Sigma$ is the surface brightness) slope in the inner region (see also the discussion in Balmaverde & Capetti 2005). Clearly, this is because in this case the "background" measured at a distance of $\sim 0.4''$ is a good estimate of the stellar emission at the center of the nucleus. On the other hand, for both "power-law" ellipticals and spirals bulges, the profile in the innermost regions (i.e. in the central 1-2 arcsec) is significantly steeper ($\gamma \sim 0.8$). In this latter case, the measurement and even the identification of faint nuclei is more difficult, because a "peaked" brightness profile of the bulge may hamper the detection of the central emission from the AGN. Furthermore, for the IR images, which have a lower angular resolution, the background cannot be measured close enough to the center of the nucleus, and thus may be significantly underestimated. We find that this would lead to overestimate the nuclear flux by a factor as large as $\sim 5$. Thus, while we used this method to measure the nuclear flux in the F330W image (aperture correction was taken into account, following the prescriptions given in Sirianni et al. 2005), we had to adopt a different strategy for the WFPC2 and NICMOS images.

2) An alternative approach consists in deriving the radial brightness profile of the galaxy, and measure any nuclear excess. Multiple component models are often used to reproduce the central regions of galaxies and measure the flux of nuclear sources (see e.g. the discussion in Quillen et al. 2001). But since here we are not interested in modeling the galaxy bulge on large scales, we only derive the radial brightness profile in the central $\sim 2$ arcsec. Then we produce a model galaxy with the same slope as observed in the region $R > 0.2$ arcsec and we assume that the profile can be extrapolated to the center of the bulge, all the way to $R = 0$. As shown in Fig. 3 (solid line), the effect of the finite resolution of HST ($\sim 0.1$ arcsec) produces a flattening of the observed profile, at a distance of $\sim 0.15$ arcsec. The observed profile, obtained by fitting ellipses to the galaxy image using the *IRAF* task *ellipse*, shows a significant excess (filled circles). We produce synthetic PSF's using the *TinyTim* software (Krist 1995), which, for WFCPC2, produces an accurate representation of the central region of the PSF, thus appropriate for our purpose. We align the synthetic PSF's with the position of the nucleus, we multiply the PSF image by an appropriate constant $K$ and we subtract the two images. We change the value of $K$ until the profile of the nuclear regions do not produce a "hole" at the center of the galaxy. The obtained profile is shown in Fig. 3 as the empty circles. To convert the flux of the nucleus from counts to physical units, we multiply the count rate ($CR = K/t_{\rm exp}$) by the keyword *PHOTFLAM* in the image header (for NICMOS $CR = K$). In Fig. 3 we also show the radial profiles obtained by subtracting PSFs that are 20% brighter and 20% fainter than our

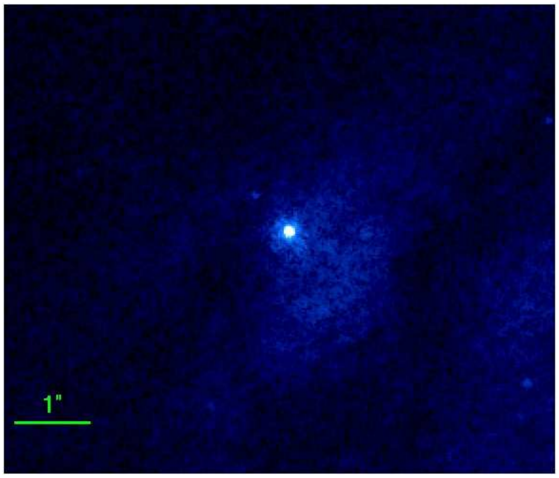

FIG. 2.— HST ACS/HRC image in the U-band (F330W filter). North is up, East is left (left panel).

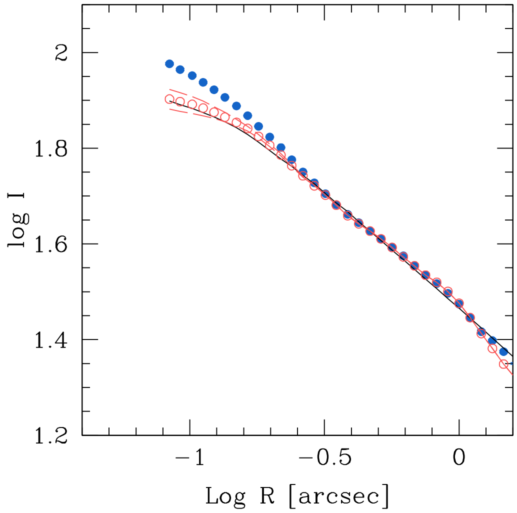

FIG. 3.— Radial brightness profiles of the central ∼ 1 arcsec of the galaxy used to measure the flux of the nuclear unresolved component. The filled circles are the observed profile (from the F814W image), the solid line is the model galaxy convolved with the HST resolution. The empty circles are the derived profile once that the nuclear component has been subtracted (see text for details). The two dashed lines are obtained subtracting PSFs that are 20% brighter and 20% fainter than the flux we report in Table 1. The errors on the profiles are of the order of or smaller than the size of the dots.

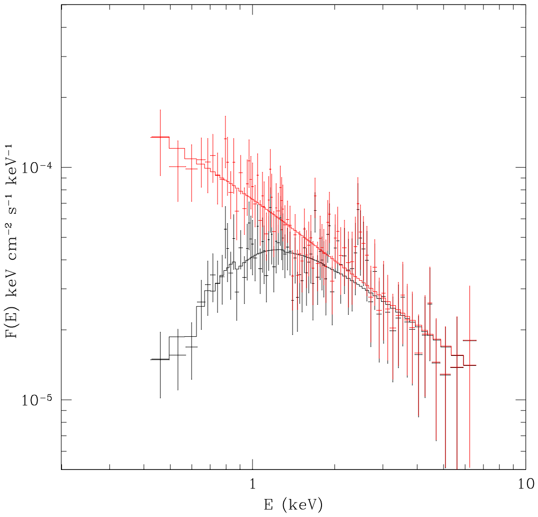

FIG. 4.— X-ray spectrum from Chandra data. The lower data-points and solid line correspond to the absorbed data and model outlined in text. The upper data-points and solid line correspond to the unabsorbed data and model.

reference value.

It is not straightforward to estimate the error on the flux measurements obtained using method 2, because the main uncertainty is the assumption that the radial profile of the galaxy can be extrapolated all the way to the center, at R=0. After subtracting synthetic PSFs with different total counts and comparing the resulting profiles with our model profile, we prefer to adopt a rather conservative value of ∼ 20% for the error of the IR and optical fluxes. With future observations, which should be taken using a dithering strategy aimed at improving the PSF sampling, the error could be significantly reduced. The statistical error on the F330W flux (obtained with method 1) is 7%. A summary of the photometry is given in Table 1.

The F450W and F555W filter pass bands include relatively strong emission lines (mainly [OIII]5007 and H$\beta$). However, since the pass bands are ∼ 1000Å wide, the observed flux is likely to be dominated by continuum emission (see also Sect. 3).

Since the near-IR and the U-band images were not taken simultaneously to the optical data, the SED may be affected by variability. We checked for variability of the nuclear source in the optical (F814W and F450W), for which two sets of observations with the same filters, taken at a distance of ∼ 1 year, are available. The nuclear fluxes are consistent within the errors, thus no variability is found between the 2 observations. However, our estimated 20% error on the optical fluxes does not allow us to exclude variations of smaller amplitude, as observed in other LLAGN (Maoz et al. 2005).

## 3. RESULTS AND DISCUSSION

### 3.1. *The nuclear SED of NGC 4565*

The absorption corrected nuclear spectral energy distribution is shown in Fig. 5. The HST data are dereddened using $N_H = 2.5 \times 10^{21}$ cm$^{-2}$, which converts to $A_V = 1.25$, assuming Galactic gas-to-dust ratio. Although in AGN the gas-to-dust ratio may differ from the local value, we believe that this choice is justified in the case of NGC 4565. As it is clear from the large field of view image of the galaxy (Fig. 1), this is a spiral seen almost edge on. Therefore, it is reasonable to assume that a significant amount of dust and gas in the disk of the galaxy project on our line-of-sight to the nucleus.

Assuming a circular geometry, from the observed ellipticity of the disk in the image we find that the orientation of the disk is likely not to exceed ∼ 10°. For comparison, we can check the absorption we find in our Galaxy for 10° Galactic Latitude. We obtain $A_V \sim 1.0 - 1.5$, where the lower value is found for Galactic longitude ∼ 180°, the higher value is for ∼ 0° (from NED). These values may actually increase substantially if we observe the same Galactic Latitude from the Galaxy center. This simple check shows that the absorption we measure in the X-rays is compatible with that provided by galactic dust

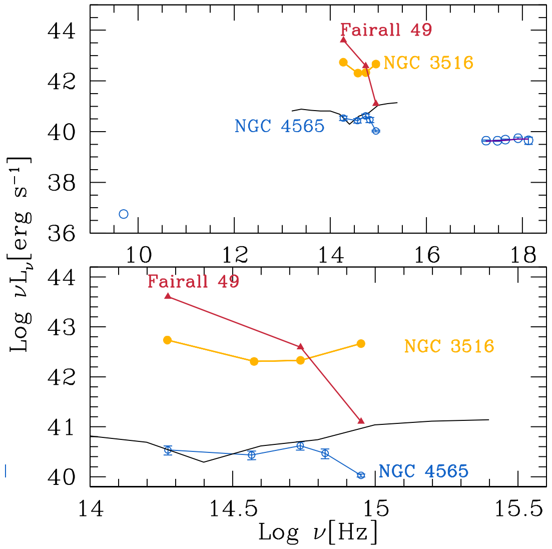

FIG. 5.— Absorption corrected nuclear spectral energy distribution of NGC 4565 from the radio to the X-ray band. The X-ray spectrum has been significantly re-binned to improve the clarity of the figure. The solid line superimposed to the X-ray data is the spectral model used to fit the data (see text). For comparison, we show the IR-to-UV SED of a Seyfert 1 (NGC 3516) and of a Compton-thin Seyfert 2 (Fairall 49). The solid line is the average SED of radio-quiet QSO from Elvis et al. (1994), normalized to the flux of NGC 4565 in the F814W filter. The lower panel is a zoom into the IR-to-UV spectral region.

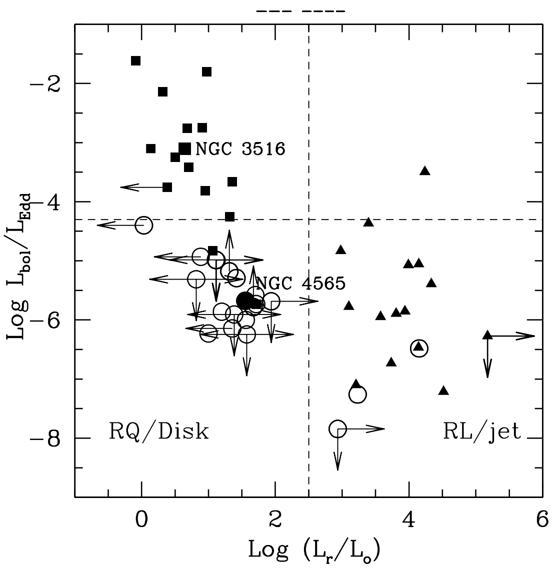

FIG. 6.— Optical to Eddington luminosity ratio plotted against the radio to optical ratio (the "nuclear radio-loudness") for the sample of nearby LLAGN (adapted from Chiaberge et al. 2005). Seyfert 1s are plotted as squares, low luminosity radio galaxies are triangles, LINERs are empty circles. NGC 4565 (filled circle) and NGC 3516 (large square) are also marked in the figure. The dashed lines are only used to guide the eye and divide objects of high and low Eddington ratio (top and bottom of the figure) and radio-quiet (disk-dominated nuclei, left) or radio loud (jet dominated nuclei, right).

in the disk. This supports our hypothesis that the moderate absorption observed to the nucleus of NGC 4565 is not produced locally, in the vicinity of the nucleus. In this case, Galactic dust-to-gas ratio may be used to convert $N_H$ derived from the X-rays to optical $A_V$.

The nuclear SED appears basically flat ($\alpha \sim 1$, $F_\nu \propto \nu^{-\alpha}$) from the 1.6$\mu$m to 4500 Å, with possibly a small peak between 5000 and 4000 Å and a small drop-off in the U-band. This peak may be real, or due to a possible contamination from emission lines (mainly [OIII] and H$\beta$) that fall in the F555W and F450W filters pass bands. Unfortunately, since neither images with narrow-band filter nor nuclear spectra are available to date, a certain ambiguity persists. However, all other filters are free from strong lines, thus the intrinsic SED cannot be dramatically different from what we show here. Whatever the nature of such a small peak, it is clear that neither a significant UV bump nor IR thermal emission from hot dust, which are characteristic of AGNs, are visible in NGC 4565. Furthermore, note that the luminosity in the X-ray is not higher than in the optical, even after absorption has been taken into account (see Fig. 4).

For comparison, in Fig. 5 we show the nuclear SED of two specific objects, together with the average SED of radio-quiet QSO as taken from Elvis et al. (1994). The two objects are a Seyfert 1 galaxy (NGC 3516) and of a Seyfert 2 (Fairall 49), for which the absorption, estimated from X-ray observations, is $N_H = 1.4 \times 10^{22}$ (Iwasawa et al. 2004). These two Seyferts have similar bolometric luminosity, but they are both clearly more powerful than NGC 4565, by $\sim$ 3 orders of magnitude. The Type 1 object clearly shows a concave spectrum, which is interpreted as the signature of the presence of the blue bump in the UV and of dust heated by the central AGN in the near-IR. The Type 2 galaxy, instead, is very bright in the IR, while the flux is dramatically reduced for higher (optical) frequencies, as a result of absorption.[4] Not all Seyferts show such a clear behavior, but these objects serve as good examples to be compared with the peculiar SED of NGC 4565.

### 3.2. *A low radiative efficiency accretion disk*

How do we interpret the nuclear emission in NGC 4565? As pointed out in the introduction, the source is included in the sample of both Merloni et al. (2003) and Falcke et al. (2004). The object does not appear to show any peculiarity, and its location along the "fundamental plane of black hole activity" does not provide us with information on the emission process. Therefore, in order to answer the above question, we use diagnostics introduced by Chiaberge et al. (2005). As already mentioned in Section 1, we found that the radio to optical nuclear luminosity ratio (i.e. the "nuclear radio-loudness") $L_r/L_o$ for LLAGNs gives us important information on the nature of the source. In particular, we can infer whether we are observing synchrotron emission in both bands (if $\log(L_r/L_o) \sim 3$), or in the optical we have some kind of excess radiation which, in the case of unabsorbed Seyferts is most likely interpreted as radiation from the accretion process. Furthermore, when the optical luminosity to Eddington luminosity ratio $L_o/L_{Edd}$ is plotted against the nuclear radio loudness (Fig. 6) different classes of LLAGNs nicely separate into three different regions of the diagram. Seyfert nuclei with relatively high accretion efficiency objects occupy the top-left part of the diagram ($L_o/L_{Edd} \sim 10^{-2} - 10^{-3}$ and $\log(L_r/L_o) \sim 1$); LINERs separate into two subclasses, which we named according to their nuclear radio-optical ratio as "radio–quiet" LINERs (bottom-left side, $L_o/L_{Edd} < 10^{-4}$ and $\log(L_r/L_o) \sim 1$), and "radio–loud" LINERS (bottom-right); radio galaxies (bottom-right part of the diagram) have the same Eddington ratio as for radio–quiet LINERs, but a much higher $\log(L_r/L_o)$. Note that in the plane of Fig. 6, the objects in which we observe an extra-component in the optical, in excess of synchrotron emission, are those that lie on the left side. Therefore, those are the objects in which emission from the accretion process can be detected. In fact, in perfect agreement with the shape of its SED, NGC 3516 lies in top-left panel of the plane, where relatively high efficiency accretion disks are. On the other hand, we did not mark the location of the Seyfert 2 galaxy Fairall 49 on the plot of Fig. 6, since the nuclear emission is most likely to be affected by significant obscuration. However, we point out that assuming that the IR flux can be used as instead of the optical, the radio to IR ratio would be similar to the Seyfert 1s in the plot (at $\log L_r/L_o = 0.88$).

---

[4] It might seem surprising to detect the nucleus in Fairall 49, which is a Seyfert 2 absorbed by a large amount of $N_H$ in the X-rays. In fact, if converted to $A_V$ using standard Galactic dust-to-gas ratio, this would correspond to 7 mag extinction in V and 11.5 mag in the F330W filter. Two possible explanations have been proposed: i) part of the optical nuclear flux in Fairall 49, if not all, might not be radiation from the accretion disk seen directly (through a moderate amount of dust). Instead, the nucleus might be in part (or completely) obscured in the optical-to-UV band, and the bulk of the observed emission may be scattered light; ii) the properties of the circumnuclear absorber are different from the Galactic dust and this would result in a non-standard $A_V/N_H$ ratio. This has been discussed by various authors (e.g. Granato et al. 1997; Maiolino et al. 2001).

Let us explore how this applies to NGC 4565. First of all, we calculate the ratio between the nuclear radio flux and the optical flux. Nagar et al. (2005) measured a radio core flux of 3.2 mJy, which implies that $\log(L_r/L_o) = 1.6$. Therefore, NGC 4565 has an excess in the optical of at least 2 dex with respect to the expected synchrotron emission (i.e. the optical counterpart of the radio core should be $>$ 2 dex fainter than the measured optical flux, unless the radio-to optical spectral index has unreasonable values for synchrotron radiation). Thus it is reasonable to interpret the optical nucleus as radiation from the accretion process. In this case, assuming a central black hole mass of $2.8 \times 10^7 M_\odot$, as derived from the M-$\sigma$ relation of Tremaine et al. (2002), and using $\sigma$ value from the LEDA database[5], the resulting Eddington ratio $L_o/L_{Edd}$ is extremely low, $2 \times 10^{-6}$. It is important to note that in the case of "typical" Seyferts, which show a blue bump, a significant bolometric correction is needed (however, this should not exceed a factor of $\sim 15$). For NGC 4565 a big blue bump is clearly not present, thus our value of $L_o$ is a good estimate of $L_{bol}$.

In the diagnostic diagram of Fig. 6, NGC 4565 lies in the lower-right quadrant, among "radio-quiet" LINERs (the other two Seyferts in the same region of the plot are M 81 and NGC 4639, as discussed in Chiaberge et al. 2005). In order to reconcile NGC 4565 with other Seyferts, which are confined in the top-left quadrant, the central black hole mass would have to be at least a factor of $\sim 100$ lower. This would substantially violate the $M_{BH} - \sigma$ relation. We conclude that the nucleus of NGC 4565 is a very low-efficiency accretion object and that we are observing the accretion process directly in the optical. This is extremely important since models of advection-dominated accretion flows are particularly sensitive to the optical-UV spectral region. For example, as shown by Quataert & Narayan (1999) the presence of winds in the disk can dramatically change the shape of the observed SED in the range of frequencies between $\nu \sim 10^{13}$ Hz and $\nu \sim 10^{15}$ Hz. However, a detailed comparison with a set of models is beyond the scope of this paper. RIAF models are very sensitive to many different physical parameters, therefore detailed modeling is useful only if the SED is well determined, from the radio-mm to the X-ray band and, if possible, when simultaneous data are available.

A similar study of the nuclear emission has been performed by Moran et al. (1999) for NGC 4395, "the least luminous Seyfert 1". In that case, the nuclear luminosity is even lower than in NGC 4565, but the central black hole mass in NGC 4395 is dramatically lower. A recent estimate based on reverberation mapping gives a value of $M_{BH} = 3.6 \times 10^5 M_\odot$ (Peterson et al. 2005). Such a low black hole mass implies $L_{bol}/L_{Edd} \sim 10^{-3}$ or higher if, as Moran et al. (1999) point out, intrinsic nuclear absorption is present. This seems in fact to be the case since (Moran et al. 2005) obtain $N_H \sim 10^{22}$ cm$^{-2}$ analyzing *Chandra* data, although most of the absorption might be produced by ionized gas. Therefore, although it is clear that even if NGC 4395 displays peculiar characteristics, its Eddington ratio is not different from the average of low luminosity Seyferts in the Palomar and CfA samples (Chiaberge et al. 2005; Ho 2004). Instead, NGC 4565 has completely different physical properties, as appears from its extremely low value of the Eddington ratio, and it is a perfect candidate for hosting a radiative inefficient accretion process.

### 3.3. *Where is the narrow line region in NGC 4565?*

One further implication of the observations we present here is worth mentioning. The flux of the [OIII]5007 emission line ($F_{[OIII]} = 1.5 \times 10^{-14}$ erg s$^{-1}$ cm$^{-2}$), as measured from the ground with a 2" beam size (Ho et al. 1997a), and the diagnostic line ratios are typical of Seyfert galaxies. Even considering the interesting (although only slightly different) classification scheme for LLAGN proposed by Kewley et al. (2006) based on SDSS data, NGC 4565 still falls in the region occupied by Seyferts. However, if we assume that all of the [OIII] flux is produced in the unresolved nucleus, this would result in a count rate higher by factor of 5 and 20 than we measure in the nucleus in the F555W and F450W, respectively. This implies that the narrow emission line region (NLR) must be extended. It is particularly interesting to investigate the properties of the NLR relatively to the nuclear properties, since it is sometimes assumed that radiative inefficient accretion cannot provide a sufficient photon field to ionize the surrounding medium and create the NLR. If this is true, we can speculate that NGC 4565 may have recently transitioned from a relatively high-efficiency accretion state (as in "normal" Seyferts) to a very low-efficiency accretion process. This might also reconcile its classification as Seyfert with the fact that its nucleus is located among LINERs in the plane of Fig. 6. The spectral classification is in fact based on the large-scale properties of the emission-line gas, that may still be powered by a higher radiation field (possibly having also a different spectral shape), because of light travel time effects. However, the equivalent width of the [OIII] line, as measured with respect to the nuclear continuum emission, is $EW_{[OIII]} \sim 100$Å. This value is in the range normally spanned by Type 1 AGN (see e.g. Kinney et al. 1991; Chiaberge et al. 2002; Marziani et al. 2003). Therefore, this may indicate that the continuum emission from RIAFs is sufficient to account for the observed [OIII] flux, and Seyferts' NLR can be powered by radiatively inefficient accretion flows. However, in the scenario in which the accretion disk has changed its state, $EW_{[OIII]}$ may assume a low value if only a fraction of the NLR gas is still highly ionized under the effect of the "past" high–efficiency state of the accretion. Clearly, only high spatial-resolution images with narrow band filters, and nuclear spectra, can provide further information to understand the recent history and ionizing mechanism of both the nucleus and NLR of NGC 4565.

---

[5] http://leda.univ-lyon1.fr/

## 4. SUMMARY AND CONCLUSIONS

We have derived the spectral energy distribution of a peculiar low-luminosity Seyfert 2 galaxy which, despite its spectral classification, basically shows no evidence for local nuclear absorption. The SED is peculiar, as it is almost flat in a $\log\nu - log(\nu F\nu)$ representation, with no sign of both a UV bump and thermally reprocessed IR emission. The very low luminosity of the source associated with a relatively high central black hole mass imply an extremely small value of the Eddington ratio ($L_o/L_{Edd} \sim 10^{-6}$). This, together with the position occupied by this object on diagnostic planes for low luminosity AGN, represents clear evidence for a low radiative efficiency accretion process at work in the innermost regions of NGC 4565. The direct detection of optical emission from such radiative inefficient processes is particularly important for providing constraints to ADAF models or similar. NGC 4565 is therefore a perfect candidate for studying RIAFs, and more observations aimed at achieving a complete coverage of the SED, from the radio-mm to the X-ray bands, should be taken in order to test the models. As part of a "search for RIAFs in LLAGN", it would also be extremely useful to derive the SED of objects that are located in the same region of the diagnostic planes as NGC 4565.

The fact that the [OIII] emission line flux is substantial in this object implies that an extended narrow line region, similar to other Seyfert galaxies, is still present in NGC 4565. A possible intriguing scenario is that the active nucleus has recently "turned-off", switching from a high efficiency, standard, accretion disk, to a radiative inefficient accretion process. However, since the EW of the [OIII]5007 emission line is rather small, with the present data we cannot rule out that the amount of ionizing photons from the RIAF is sufficient to produce the observed [OIII] flux.

We thank the anonymous referee for her/his comments that greatly improved the paper. We acknowledge Dave Axon, Alessandro Capetti and Alice Quillen for useful comments. RG acknowledges support from the STScI Visitor Program.

This research has made use of the NASA/IPAC Extragalactic Database (NED) which is operated by the Jet Propulsion Laboratory, California Institute of Technology, under contract with the National Aeronautics and Space Administration.

*Facilities:* HST, Chandra.

## REFERENCES

Abramowicz, M. A., Igumenshchev, I. V., Quataert, E., & Narayan, R. 2002, ApJ, 565, 1101
Balmaverde, B., & Capetti, A. 2006, A&A, 447, 97
Bregman, J. N. 2005, ArXiv Astrophysics e-prints, astro-ph/0511368
Cappi, M., et al. 2006, A&A, 446, 459
Chiaberge, M., Capetti, A., & Celotti, A. 1999, A&A, 349, 77
—. 2002, A&A, 394, 791
Chiaberge, M., Capetti, A., & Macchetto, F. D. 2005, ApJ, 625, 716
Di Matteo, T., Allen, S. W., Fabian, A. C., Wilson, A. S., & Young, A. J. 2003, ApJ, 582, 133
Di Matteo, T., Quataert, E., Allen, S. W., Narayan, R., & Fabian, A. C. 2000, MNRAS, 311, 507
Dickey, J. M., & Lockman, F. J. 1990, ARA&A, 28, 215
Elvis, M., et al. 1994, ApJS, 95, 1
Faber, S. M., et al. 1997, AJ, 114, 1771
Falcke, H., Körding, E., & Markoff, S. 2004, A&A, 414, 895
Foschini, L., et al. 2002, A&A, 392, 817
Granato, G. L., Danese, L., & Franceschini, A. 1997, ApJ, 486, 147
Ho, L. C. 2004, in Multiwavelength AGN Surveys, 153
Ho, L. C., Filippenko, A. V., & Sargent, W. L. W. 1997a, ApJS, 112, 315
Ho, L. C., Filippenko, A. V., Sargent, W. L. W., & Peng, C. Y. 1997b, ApJS, 112, 391
Iwasawa, K., Lee, J. C., Young, A. J., Reynolds, C. S., & Fabian, A. C. 2004, MNRAS, 347, 411
Kewley, L. J., Groves, B., Kauffmann, G., & Heckman, T. 2006, ArXiv Astrophysics e-prints, astro-ph/0605681
Kinney, A. L., Antonucci, R. R. J., Ward, M. J., Wilson, A. S., & Whittle, M. 1991, ApJ, 377, 100
Koerding, E., Falcke, H., & Corbel, S. 2006, ArXiv Astrophysics e-prints, astro-ph/0603117
Krist, J. 1995, in ASP Conf. Ser. 77: Astronomical Data Analysis Software and Systems IV, 349–+
Maiolino, R., Marconi, A., & Oliva, E. 2001, A&A, 365, 37
Maoz, D., Nagar, N. M., Falcke, H., & Wilson, A. S. 2005, ApJ, 625, 699
Marziani, P., Sulentic, J. W., Zamanov, R., Calvani, M., Dultzin-Hacyan, D., Bachev, R., & Zwitter, T. 2003, ApJS, 145, 199
Merloni, A., Heinz, S., & di Matteo, T. 2003, MNRAS, 345, 1057
Moran, E. C., Eracleous, M., Leighly, K. M., Chartas, G., Filippenko, A. V., Ho, L. C., & Blanco, P. R. 2005, AJ, 129, 2108
Moran, E. C., Filippenko, A. V., Ho, L. C., Shields, J. C., Belloni, T., Comastri, A., Snowden, S. L., & Sramek, R. A. 1999, PASP, 111, 801
Nagar, N. M., Falcke, H., & Wilson, A. S. 2005, A&A, 435, 521
Narayan, R., & Yi, I. 1994, ApJ, 428, L13
Pavlosky, C. e. a. 2005, ACD Data Handbook, Version 4.0, (Baltimore: STScI)
Peterson, B. M., et al. 2005, ApJ, 632, 799
Quataert, E., & Narayan, R. 1999, ApJ, 520, 298
Quillen, A. C., McDonald, C., Alonso-Herrero, A., Lee, A., Shaked, S., Rieke, M. J., & Rieke, G. H. 2001, ApJ, 547, 129
Rees, M. J., Phinney, E. S., Begelman, M. C., & Blandford, R. D. 1982, Nature, 295, 17
Sirianni, M., et al. 2005, PASP, 117, 1049
Tremaine, S., et al. 2002, ApJ, 574, 740